

## Co-occurrence of *Alexandrium minutum* (Dinophyceae) ribotypes from the Chinese and Malaysian coastal waters and their toxin production

Minlu Liu<sup>a</sup>, Bernd Krock<sup>b</sup>, Rencheng Yu<sup>c</sup>, Chui Pin Leaw<sup>d</sup>, Po Teen Lim<sup>d</sup>, Guangmao Ding<sup>e</sup>, Na Wang<sup>a</sup>, Jing Zheng<sup>a</sup>, Haifeng Gu<sup>a,f,g,\*</sup>

<sup>a</sup> Third Institute of Oceanography, Ministry of Natural Resources, Xiamen 361005, China

<sup>b</sup> Alfred Wegener Institut–Helmholtz Zentrum für Polar- und Meeresforschung, Am Handelshafen 12, Bremerhaven, D–27570 Germany

<sup>c</sup> CAS Key Laboratory of Marine Ecology and Environmental Sciences, Institute of Oceanology, Chinese Academy of Sciences, Qingdao 266071, China

<sup>d</sup> Bachok Marine Research Station, Institute of Ocean and Earth Sciences, University of Malaya, 16310 Bachok, Kelantan, Malaysia

<sup>e</sup> Fishery Resources Monitoring Center of Fujian Province, Fuzhou 350003, China

<sup>f</sup> Key Laboratory of Marine Ecological Conservation and Restoration, Ministry of Natural Resources, Xiamen 361005, China

<sup>g</sup> Fujian Provincial Key Laboratory of Marine Ecological Conservation and Restoration, Xiamen 361005, China

### ARTICLE INFO

Editor Dr. C. Gobler

#### Keywords:

Cryptic species  
Dinoflagellates  
Harmful algal bloom (HAB)  
Metabarcoding  
Paralytic shellfish toxins (PSTs)

### ABSTRACT

The bloom-forming dinophyte *Alexandrium minutum* comprises biogeographic inferred, global and Pacific clades with both toxic and nontoxic strains reported. *A. minutum* has a wide distribution in the Western Pacific, but to date only a few strains have available DNA sequences. To fully understand its genetic diversity, sampling was undertaken from the Yellow Sea, the East and South China Sea, and five strains of *A. minutum* and two strains of its sister species, *A. tamutum*, were established. Their morphology was examined by light and scanning electron microscopy. In addition, sequences were obtained from both large subunit (LSU) ribosomal DNA and/or internal transcribed spacer (ITS) region. Strains of *A. minutum* are morphologically indistinguishable, characterized by a smaller cell size and a narrow sixth precingular plate. In contrast, *A. tamutum* has a wider sixth precingular plate. High nucleotide divergences of LSU (D1–D3) rDNA and ITS were revealed amongst strains of *A. minutum* (10% and 25%, respectively), and *A. tamutum* (3% and 13%, respectively). Molecular phylogenies based on LSU rDNA and ITS revealed three ribotypes (B–D) of *A. minutum*, and two ribotypes of *A. tamutum* in the Western Pacific. Seasonal sampling in the East China Sea to detect *A. minutum* using the DNA metabarcoding targeting ITS1 region was also performed. Our results showed that the ribotypes B and C of *A. minutum* co-occurred in the water. Paralytic shellfish toxin (PSTs) of all seven strains was analysed using liquid chromatography with tandem mass spectrometry (LC–MS/MS). PSTs were detected only in *A. minutum* ribotypes B and C with predominance of gonyautoxins 1/4. Our results suggest high diversity and risk potential of this toxic species in this region.

### 1. Introduction

The dinophyte genus *Alexandrium* Halim encompasses 33 taxonomically accepted species (Guiry and Guiry, 2022) and many of them are toxic and bloom forming (Anderson et al., 2012). The type species of *Alexandrium*, *A. minutum* Halim was originally described from the Alexandria Harbour, Egypt (Halim, 1960). Its morphological details, however, remained unclear until the re-description of materials from the type locality (Balech, 1989). Prior to this, many *Alexandrium* species were classified within *Gonyaulax* Diesing, including *G. tamarensis* Lebour (Lebour, 1925), and *G. catenella* Whedon & Kofoid (Whedon and Kofoid, 1936). Once the identity of *A. minutum* was settled, *Gonyaulax tamarensis*

was transferred into *Alexandrium* as *A. tamarensis* (Lebour) Balech together with many other species (Balech, 1995).

The taxonomic criteria to differentiate *Alexandrium* species are subtle; these include size and shape of cells, the connection between the first apical plate and apical pore complex, the shape of the first apical plate, presence or absence of the ventral pore, the shape of the sixth precingular plates, anterior and posterior sulcal plates (Balech, 1995). *A. tamarensis*, *A. catenella* (Whedon & Kofoid) Balech and *A. fundyense* Balech are three morphologically similar species and used to form the *A. tamarensis* species complex. Recently, these species were redefined and five species were identified based on evidence from morphological, molecular and crossing data (John et al., 2014; Fraga et al., 2015).

\* Corresponding author.

E-mail address: [guhaifeng@tio.org.cn](mailto:guhaifeng@tio.org.cn) (H. Gu).

<https://doi.org/10.1016/j.hal.2022.102238>

Received 6 January 2022; Received in revised form 3 April 2022; Accepted 14 April 2022

Available online 22 April 2022

1568-9883/© 2022 Elsevier B.V. All rights reserved.

Likewise, several other *Alexandrium* species that are morphologically similar to *A. minutum* have been described; these included *A. andersonii* Balech, *A. lusitanicum* Balech, *A. angustitabulatum* FJR Taylor, and *A. tamutum* Montresor, Beran & John. Both *A. lusitanicum* and *A. angustitabulatum* were considered to be junior synonyms of *A. minutum*, since the characters used to differentiate these species including the length: width of the anterior sulcal plate, and the presence of a ventral pore were found to be plastic within a population, while *A. tamutum* and *A. andersonii* were proven as separate species (Hansen et al., 2003; Lilly et al., 2005). Currently, two biogeographically distinct clades of *A. minutum* have been identified, i.e., the global clade and Pacific clade, based on the ribosomal DNA sequences; the global clade comprises strains exclusively from Europe and Australia, while the Pacific clade includes strains from Taiwan and New Zealand (Lilly et al., 2005).

Paralytic shellfish toxin (PST) production of *A. minutum* was firstly reported from several Australian strains, which mainly produced gonyautoxins 1–4 (GTX1–4) (Oshima et al., 1989). Most strains of *A. minutum* from Asian Pacific produced carbamoyl toxins (GTX1–4), neosaxitoxin (NEO), and saxitoxin (STX) (MacKenzie and Berkett, 1997; Hwang et al., 1999; Lim and Ogata, 2005; Lim et al., 2006, 2007, 2010), but strains from Denmark produced predominantly *N*-sulfocarbamoyl toxins (C1/2) (Hansen et al., 2003). In contrast, some strains from Ireland, UK, Italy, and Taiwan, which belong to either the global or Pacific clade, were found to be nontoxic (Lilly et al., 2005; Touzet et al., 2007; Brown et al., 2010; Yang et al., 2010). Globally, strains of *A. minutum* can be divided into five groups based on their toxin profiles; some of them have limited biogeography but others have a much wider distribution (Lewis et al., 2018).

*Alexandrium minutum* has often been found in sheltered embayments and estuaries. Blooms of *A. minutum* have been reported in the Alexandria Harbour, Egypt (Halim, 1960), in Port River, Adelaide, Australia (Hallegraeff et al., 1988), Mediterranean Sea (Delgado et al., 1990; Vila et al., 2005; Bravo et al., 2008; Abdenadher et al., 2012). Cape Town Harbour, South Africa (Pitcher et al., 2007), the Azores Archipelago (Northeastern Atlantic Ocean) (Santos et al., 2014), Bay of Brest and English Channel, France (Chapelle et al., 2015; Guallar et al., 2017), and Kingston Harbour, Jamaica (Ranston et al., 2007). In the Asian Pacific, blooms formed in aquaculture ponds of Lianyungang (Yellow Sea) and southern Taiwan (Su and Chiang, 1991; Tang et al., 2012), and lagoons of Peninsular Malaysia (Lim et al., 2004; Lau et al., 2017).

In addition to these bloom events, *A. minutum* displays a wider biogeography in the Asian Pacific, recorded in Japan, Korea, Daya Bay, China, Vietnam, northeast coast of Peninsular Malaysia, Gulf of Thailand, and Philippines (Yuki, 1994; Yoshida et al., 2000; Piumsomboon et al., 2001; Usup et al., 2002; Park and Kang, 2009; Baula et al., 2011; Liu et al., 2021b). However, molecular sequences of strains from this region are limited and all available strains fell within the Pacific clade (Lilly et al., 2005). In contrast, strains from Taiwan showed the highest variability in toxin profiles (Lewis et al., 2018), although strains from mainland China, Vietnam and Malaysia always produced predominantly GTX1–4 (Yoshida et al., 2000; Lim and Ogata, 2005; Lim et al., 2006; Liu et al., 2021b).

In view of morphological similarity amongst *Alexandrium* species, it is essential to develop molecular based approaches such as quantitative real-time PCR to quantify cells of *A. minutum* in the waters (Galluzzi et al., 2004; Touzet et al., 2007; Park and Kang, 2009). However, this approach was often designed based on sequences of a single ribotype and assuming that co-occurrence of several other ribotypes is not likely in the environment. High-throughput sequencing (HTS) targeting variable region, such as the large subunit ribosomal DNA (D1–D2), or the internal transcribed spacer (ITS1 or ITS2), has been proven to be powerful to unveil the diversity of harmful algal bloom species in the environments (Silvever et al., 2019; Fu et al., 2021), especially for those species with various ribotypes.

To fully understand the taxonomic diversity of *A. minutum* in the

Asian Pacific, we collected samples from the Yellow Sea to the South China Sea and established seven strains for detailed morphological and genetic examination. Furthermore, to test if various ribotypes of *A. minutum* co-occur, we performed seasonal sampling in two bays of the East China Sea and detected them using HTS metabarcoding method targeting the ITS1 region. All seven strains were subjected to a PST toxin analysis using liquid chromatography with tandem mass spectrometry (LC–MS/MS).

## 2. Materials and methods

### 2.1. Sample collection and treatment

Plankton samples were collected using 10  $\mu\text{m}$  mesh-size plankton net at five coastal sites in Yellow Sea, East China Sea and South China Sea between the period of 2008 and 2018 (Table 1, Fig. 1). Single *Alexandrium* cells were isolated using a micropipette with a Nikon Eclipse TS100 inverted microscope (Nikon, Tokyo, Japan), and transferred into wells of 96-well plates filled with f/2–Si medium (Guillard and Ryther, 1962). Seven strains were established and maintained in f/2–Si medium at 20 °C (sub-tropical and temperate strains) or 25 °C (tropical strains), 90  $\mu\text{E}\cdot\text{m}^{-2}\cdot\text{s}^{-1}$  under a 12:12 h light: dark cycle.

Dummy citations Tables 2, 3, 4, and 5

Water samples were collected monthly at three stations in Xiamen Harbour from May 2018 to January 2020 and occasionally at 17 stations in Dongshan Bay from May 2019 to December 2020 (Fig. 2, Supplementary Tables S1 and S2). Two liters of water samples from surface and bottom were collected and prefiltered through a 200  $\mu\text{m}$  mesh, subsequently filtered onto 5  $\mu\text{m}$  pore-size polycarbonate filters (Millipore, Eschborn, Germany), and stored at –20 °C for DNA extraction.

Sediment samples were collected at four stations in Dongshan Bay in May 2019 (Supplementary Table S2) and stored at 4°C for several months. Approximately 10 g sediment were mixed with 15 mL filtered seawater and ultrasonicated for 2 min. The samples were then sieved through 200  $\mu\text{m}$  and 10  $\mu\text{m}$  mesh and washed and collected with filtered seawater. Cysts were separated and concentrated using sodium polytungstate following Bolch (1997) for DNA extraction.

### 2.2. Morphological observation of motile cells with LM and SEM

Live cells were examined and photographed using a Zeiss Axio Imager light microscope (Carl Zeiss, Göttingen, Germany) equipped with a Zeiss Axiocam HRC digital camera. Cell size was measured using Axiovision v.4.8.2 software at 400  $\times$  magnification. Calcofluor white was used to stain thecal plates following Fritz and Triemer (1985).

Cells at exponential growing stage were concentrated by a Universal 320 R centrifuge (Hettich–Zentrifugen, Tuttlingen, Germany) at 850 g for 10 min at room temperature. Samples were fixed with 2.5% glutaraldehyde for 1 h at room temperature and were transferred to a coverslip coated with poly-L-lysine (molecular weight 70,000–150,000). The cover slip were rinsed with Milli-Q water twice and dehydrated in a graded ethanol series (10, 30, 50, 70, 90 and 3  $\times$  in 100% for 10 min at each step), then critical point dried using a K850 Critical Point Dryer (Quorum/Emitech, West Sussex, UK), sputter-coated with gold. Samples were examined with a Zeiss Sigma FE scanning electron microscope (Carl Zeiss, Oberkochen, Germany). The thecal plate tabulation follows Fensome et al. (1993) and Balech (1980).

### 2.3. Gene amplification and sequencing

The genomic DNA from each strain was extracted from 10 mL cultures using a MiniBEST Universal DNA Extraction Kit (Takara, Tokyo, Japan) according to the manufacturer's protocol. Gene amplifications were carried out in a 50  $\mu\text{L}$  reaction containing 1  $\times$  PCR buffer, 50  $\mu\text{M}$  dNTP mixture, 0.2  $\mu\text{M}$  of each primer, 10 ng of template genomic DNA, and 1 U of ExTaq DNA Polymerase (Takara, Tokyo, Japan). The LSU

**Table 1**

Information on strains of *Alexandrium minutum* and *A. tamutum* examined in this study, including the collection date, locations, and toxin production.

Species	Strains	Collection date	Origin	Latitude (N)	Longitude (E)	Toxic
<i>A. minutum</i>	TIO914	13 Apr., 2018	Quanzhou, East China Sea	24°53'1.78"	118°54'56.85"	Yes
<i>A. minutum</i>	AM-LYG	22 Jul. 2008	Lianyungang, Yellow Sea	34°48'29.28"	119°11'25.92"	Yes
<i>A. minutum</i>	BK280604	28 Jun. 2015	Pantai Melawi, Bachok, Malaysia	6°0'34.40"	102°25'35.30"	<0.048 pg cell <sup>-1</sup>
<i>A. minutum</i>	AmTm01	20 Jun. 2014	Sungai Geting, Tumpat, Malaysia	6°13'31.20"	102°6'39.30"	Yes
<i>A. minutum</i>	AmTm02	20 Jun. 2014	Sungai Geting, Tumpat, Malaysia	6°13'31.20"	102°6'39.30"	Yes
<i>A. tamutum</i>	TIO589	6 May 2018	Ningde, East China Sea	26°54'35.00"	120°20'34.00"	<0.003 pg cell <sup>-1</sup>
<i>A. tamutum</i>	BK2703S1	27 Mar. 2016	Pantai Melawi, Bachok, Malaysia	6°0'34.40"	102°25'35.30"	<0.042 pg cell <sup>-1</sup>

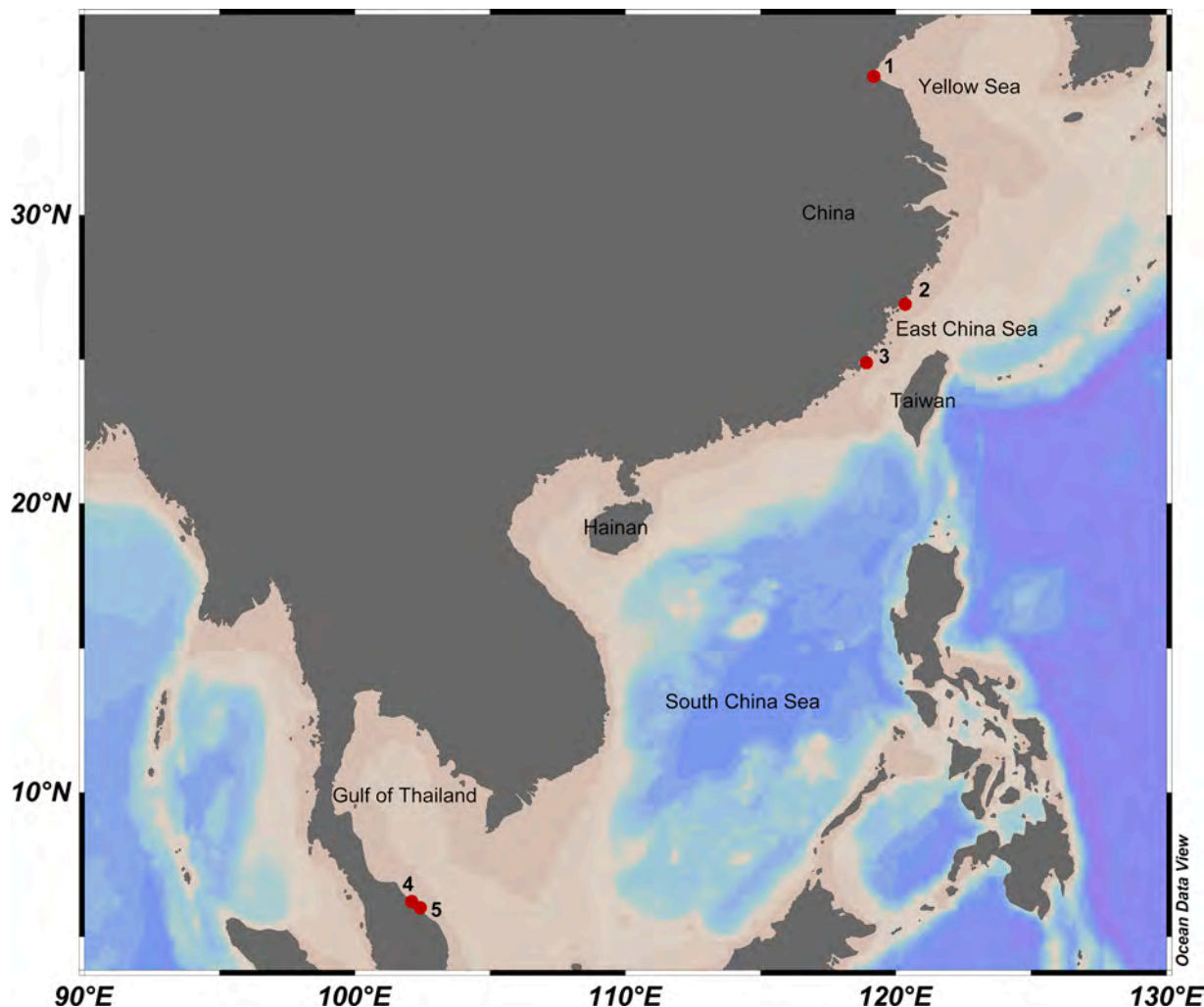


**Fig. 1.** Map of sampling stations in the South China Sea where *Alexandrium* strains were established. 1: Lianyungang, Jiangsu, China; 2: Ningde, Fujian, China; 3: Quanzhou, Fujian, China; 4: Tumpat, Malaysia; 5: Bachok, Malaysia.

**Table 2**

LSU sequence similarities of *Alexandrium minutum* and *A. tamutum* strains.

Species	Ribotypes	Strains	TIO914	BK2703S1	TIO589	EU707460	AF318233	AMLYG	BK280604
<i>A. minutum</i>	C	TIO914	–	–	–	–	–	–	–
<i>A. tamutum</i>	B	BK2703S1	91.1%	–	–	–	–	–	–
<i>A. tamutum</i>	A	TIO589	91.9%	96.6%	–	–	–	–	–
<i>A. minutum</i>	A	EU707460	93.2%	92.9%	94.5%	–	–	–	–
<i>A. insuetum</i>	NA	AF318233	91.0%	94.5%	95.8%	94.0%	–	–	–
<i>A. minutum</i>	B	AMLYG	92.5%	93.5%	94.5%	94.3%	94.0%	–	–
<i>A. minutum</i>	D	BK280604	89.6%	90.9%	91.9%	91.1%	90.8%	91.6%	–

**Table 3**ITS sequence similarities amongst *Alexandrium minutum* and related species.

Species	Ribotypes	Strains	AM-LYG	Am b	TIO589	AB006996	AOF0922	BK2703S1	TIO914	BK280604-1
<i>A. minutum</i>	B	AM-LYG	–	–	–	–	–	–	–	–
<i>A. minutum</i>	A	Am b	86.1%	–	–	–	–	–	–	–
<i>A. tamutum</i>	A	TIO589	83.2%	88.2%	–	–	–	–	–	–
<i>A. insuetum</i>	NA	S1	83.3%	87.1%	92.5%	–	–	–	–	–
<i>A. ostenfeldii</i>	NA	AOF0922	82.1%	84.2%	87.1%	86.1%	–	–	–	–
<i>A. tamutum</i>	B	BK2703S1	81.1%	85.4%	87.4%	83.6%	80.1%	–	–	–
<i>A. minutum</i>	C	TIO914	78.2%	82.6%	79.6%	80.1%	78.1%	77.9%	–	–
<i>A. minutum</i>	D	BK280604-1	75.9%	78.4%	75.4%	75.5%	74.7%	74.7%	75.6%	–
<i>A. minutum</i>	D	BK280604-7	76.7%	79.2%	76.1%	76.2%	75.4%	75.4%	76.3%	99.0%

**Table 4**Morphological comparison of *Alexandrium minutum* and *A. tamutum* strains.

Species	Ribotype	Strains	Cell length (µm)	Cell width (µm)	Ventral pore	Length:width of 6'	Reference
<i>A. minutum</i>	B	AM-LYG	18.2–30.4 (22.7 ± 2.7, n = 30)	20.2–31.4 (24.9 ± 3.0, n = 30)	Present	1.9	Present study
<i>A. minutum</i>	C	TIO914	14.4–21.7 (18.5 ± 1.8, n = 30)	18.2–26.3 (20.9 ± 1.7, n = 30)	Present	1.9	Present study
<i>A. minutum</i>	D	BK280604	14.4–22.0 (17.9 ± 1.9, n = 16)	14.9–23.0 (17.7 ± 2.1, n = 16)	Present	1.9	Present study
<i>A. minutum</i>	A?		17–29	12–24	Present	1.7–2.0	Balech, 1989
<i>A. tamutum</i>	A	TIO589	14.0–20.3 (16.0 ± 1.9, n = 12)	13.3–20.3 (15.7 ± 1.7, n = 12)	Present	0.8	Present study
<i>A. tamutum</i>	B	BK2703S1	22.2–33.5 (27.7 ± 3.5, n = 15)	21.3–31.3 (26.7 ± 2.8, n = 15)	Present	0.8	Present study
<i>A. tamutum</i>	A		19–34	19–33	Present	1.0	Montresor et al., 2004

**Table 5**Toxin production of *Alexandrium minutum* from East Asia Pacific and New Zealand, including their ribotype, strain or origin and references. +++: dominant; ++: minor; +: trace; -: not detected. NA: not available.

Species	Ribotype	Strain/origin	GTX1/4	GTX2/3	NEO	STX	References
<i>A. minutum</i>	B	AM-LYG/China	+++	++	+	+	Present study
<i>A. minutum</i>	B	AmTm01/Malaysia	+++	+	–	–	Present study
<i>A. minutum</i>	B	AmTm02/Malaysia	+++	++	–	–	Present study
<i>A. minutum</i>	C	TIO914/China	+++	+	–	–	Present study
<i>A. minutum</i>	D	BK280604/Malaysia	–	–	–	–	Present study
<i>A. minutum</i>	B	-/Daya Bay, China	–	+++	–	–	Liu et al., 2021
<i>A. minutum</i>	NA	-/Taiwan	+	+++	+	+	Hwang et al., 1999
<i>A. minutum</i>	NA	-/Taiwan	–	–	–	–	Lilly et al., 2005
<i>A. minutum</i>	NA	-/Vietnam	+++	–	–	–	Yoshida et al., 2000
<i>A. minutum</i>	NA	AmSp01/Vietnam	+++	–	+	–	Lim et al., 2007
<i>A. minutum</i>	NA	-/Thailand	+++	+	–	–	Piumsomboon et al., 2001
<i>A. minutum</i>	B	CAWD11/New Zealand	++	+++	++	+++	MacKenzie and Berkett 1997
<i>A. minutum</i>	B	CAWD13/New Zealand	+++	+	++	++	MacKenzie and Berkett 1997

rDNA (D1–D6) was amplified using the primer pair D1R/28 and 1483R (Daugbjerg et al., 2000), while the ITS region (ITS1–5.8S–ITS2) was amplified using ITSA and ITSB (Adachi et al., 1996). The polymerase chain reaction was performed using a Mastercycler (Eppendorf, Hamburg, Germany) with the thermal cycling procedure of 4 min at 94 °C, followed by 30 cycles of 1 min at 94 °C, 1 min at 45 °C, 1 min at 72 °C, and final extension of 7 min at 72 °C. The amplicons were purified using a SanPrep Column DNA Gel Extraction Kit (Sangon Biotech, Shanghai, China) and sequenced directly in both directions on an ABI PRISM 3730XL (Applied Biosystems, Foster City, CA, USA) following the manufacturer's instructions. All newly obtained sequences were deposited in GenBank (NCBI) with accession numbers ON139120 to ON139124 and ON139194 to ON139201.

#### 2.4. Sequence alignment and phylogenetic analysis

Newly obtained LSU rDNA and ITS sequences were incorporated into closely related *Alexandrium* sequences retrieved from the GenBank nucleotide database (NCBI). The nucleotide sequences were aligned using MAFFT v7.110 (Kato and Standley, 2013, <http://mafft.cbrc.jp/alignment/server/>) with the default settings. The multiple alignments were manually checked, and sequence similarity was assessed using

BioEdit v. 7.0.5 (Hall, 1999).

For Bayesian inference (BI), jModelTest (Posada, 2008) was used to select the most appropriate model with Akaike Information Criterion. Bayesian reconstruction of the data matrix was performed using MrBayes 3.2 (Ronquist and Huelsenbeck, 2003). Four Markov chain Monte Carlo chains were performed for 5000,000 generations, sampling every 1000 generations. The first 10% of burn-in trees were discarded. A majority rule consensus tree was reconstructed to examine the posterior probabilities of each clade. Maximum likelihood (ML) was performed using RaxML v.7.2.6 (Stamatakis, 2006) on the T-REX web server (Boc et al., 2012). Node support was assessed with 1000 bootstrap replications.

#### 2.5. Toxin analysis

Cells of five *A. minutum* strains and two *A. tamutum* strains in the exponential growth phase were collected ( $10^5$ – $10^7$  cells) by a Universal 320 R centrifuge (Hettich-Zentrifugen, Tuttlingen, Germany) at 2500 g for 10 min at 4 °C. Algal pellets were transferred to 2 mL microcentrifuge tubes and stored at –20 °C until analysis.

Cell pellets were resuspended in 500 µL 0.03 M acetic acid and homogenized with 0.9 g of lysing matrix D by reciprocal shaking at 6.5 m s

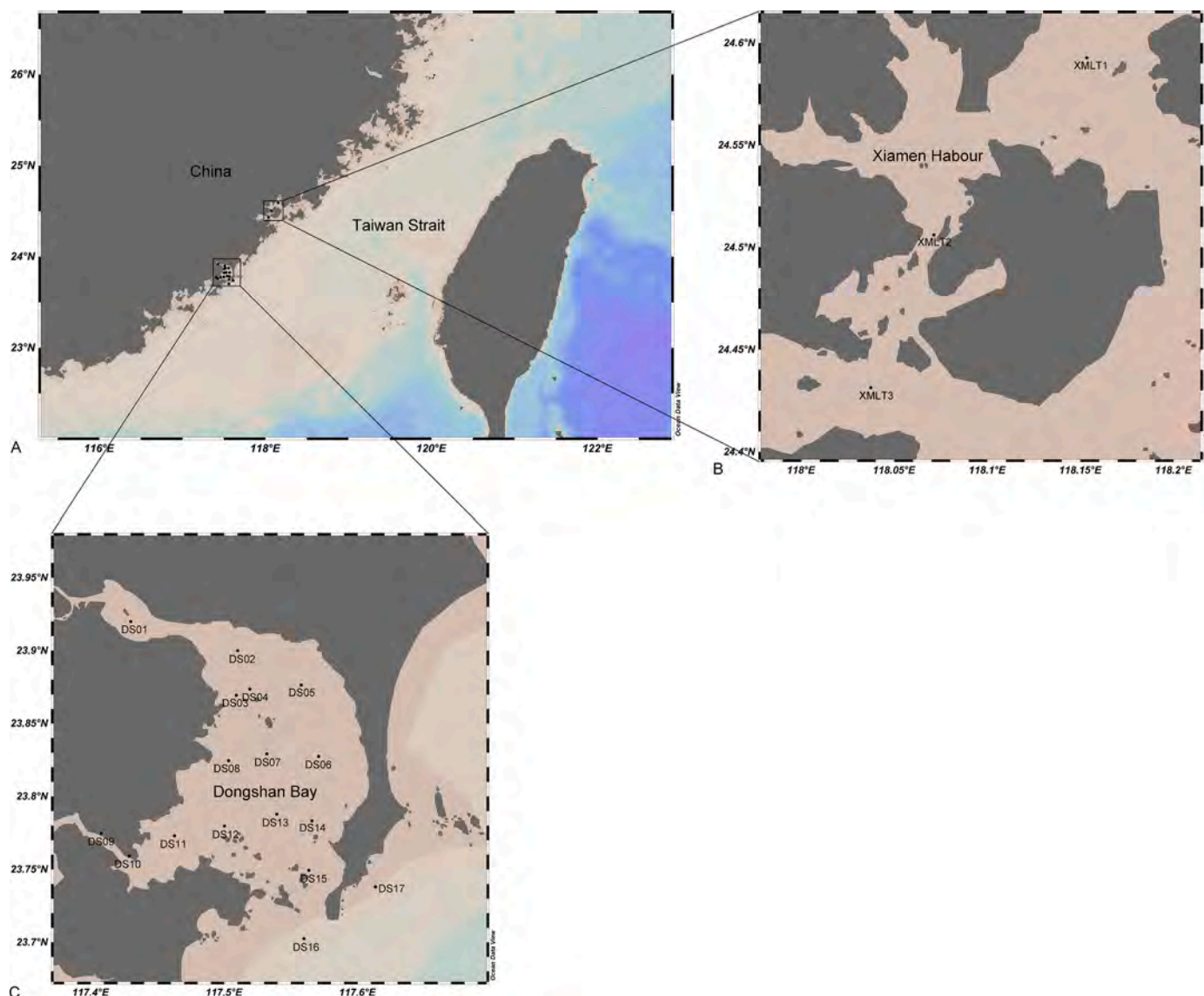


Fig. 2. Map of stations in Xiamen Harbour and Dongshan Bay (the East China Sea) where seasonal sampling was performed.

$^{-1}$  for 45 s in a Bio101 FastPrep instrument (Thermo Savant, Illkirch, France). Samples were then centrifuged at 16,100 g for 15 min at 4 °C. The supernatants were transferred to spin-filters of 0.45  $\mu$ m pore-size (Millipore Ultrafree, Eschborn, Germany) and centrifuged for 30 s at 800 g, and then transferred to autosampler vials until measurement by LC-MS/MS.

Measurements were performed in the selected reaction monitoring (SRM) mode on a Xevo TQ-XS triple quadrupole mass spectrometer equipped with a Z-Spray source (Waters, Eschborn, Germany) as described previously in detail (Liu et al., 2021a). PSTs were quantified by external calibration with standard mix solutions of four concentration levels consisting of the following PSTs: STX, NEO, GTX2/3, GTX1/4, dcSTX, dcNEO, dcGTX2/3, dcGTX1/4, B1 (GTX5), B2 (GTX6), C1/2, and C3/4 purchased from the Certified Reference Materials Program (CRMP) of the Institute for Marine Biosciences, National Research Council (Halifax, NS, Canada).

## 2.6. Environmental DNA extraction and Illumina sequencing

Genomic DNA from water and sediment samples was extracted using a NucleoSpin®Soil Kit (Macherey-Nagel, Düren, Germany) following the manufacturer's protocol. The primers PRIMER B

(5'-TAGGTGAACCTGCAGAAGGAT-3') (Medlin et al., 1988) and ITS300R (5'-CACGGAAKTTCTGCARTTCACAATG-3') (Fu et al., 2021), targeting the ITS1 of dinophytes, were used. For each sample, an identifying barcode was placed on the forward primer and a 34 cycle PCR using the Premix Taq (Takara, Dalian, China) was performed. The following PCR conditions were used: 95 °C for 5 min, followed by 34 cycles of 95 °C for 50 s, 47 °C for 50 s, and 72 °C for 50 s, and a final elongation step at 72 °C for 10 min. The library was built according to the standard protocol of NEBNext® Ultra™ DNA Library Prep Kit for Illumina® (New England Biolabs, MA, USA). The amplicons were sequenced using a HiSeq 2500 platform (Illumina, CA, USA) based on a paired-end strategy (2 × 250 bp).

The reads obtained from HiSeq sequencing were analysed using USEARCH v11.0.667 (Edgar, 2013) and VSEARCH v2.14.2 (Rognes et al., 2016). Firstly, the raw reads were assembled and merged, and the primer sequences were removed from both edges of the assembled reads. Then, the preprocessed reads were filtered, dereplicated and denoised to remove low quality reads (error rate > 1%), short reads (< 140 bp), chimeras and singleton reads (Edgar and Flyvbjerg, 2015; Rognes et al., 2016). Reads were clustered to ZOTUs (zero-radius operational taxonomic units) according to 97% similarity and the most abundant read was selected as the representative read for each ZOTU (Edgar, 2013).

Finally, ZOTUs annotation was conducted on the representative read of each ZOTUs against the in-house curated ITS database (Fu et al., 2021) updated in December 2021, with the similarity at a cutoff level of 99%. In addition, ZOTUs with coverage values less than 90% were removed. ZOTUs of each sample were randomly re-sampled to an equal sample size.

### 3. Results

Seven strains of *Alexandrium* were established in this study, five were identified as *A. minutum* and two were determined as *A. tamutum* (Table 1).

#### 3.1. Molecular characterization

##### 3.1.1. LSU rDNA (D1–D3) phylogeny

The LSU rDNA (D1–D3) sequence similarities amongst strains of *A. minutum* ranged from 89.6% to 94.3% (Table 2). The phylogenetic analyses yielded identical tree topologies by ML and BI; with the ML tree shown in Fig. 3. The resulting trees demonstrated that *A. minutum* was a sister clade of *A. insuetum* with strong supports (ML/BI, 100%/0.98). They again, formed a sister clade to *A. tamutum* with strong ML (100%) and BI (0.93) supports. *Alexandrium tamutum* consisted of two clades. One of them comprised strains BK2703S1 and AMTK-5 from Malaysia and Taiwan with maximal support (ML/BI, 100%/1.0). The other clade comprised of strain TIO589 from the East China Sea and those from Italy (ML/BI, 100%/0.90).

The end-clade of *A. minutum* was monophyletic (ML/BI, 100%/0.99), comprising four distinct clades, here referred to as ribotypes A–D (Fig. 3). Ribotype A comprised strains from the Mediterranean Sea, Atlantic Europe, Australia, and South Africa. Ribotype B consisted of strains from the Asian Pacific and New Zealand. Strain TIO914 from the East China Sea and strain BK280604 from the South China Sea fell outside these two main ribo-clades and hereafter are referred to as ribotypes C and D, respectively.

##### 3.1.2. ITS dataset and the phylogeny

The ITS sequence similarities amongst strains of *A. minutum* ranged from 75.6% to 86.1% (Table 3). The phylogenetic analyses yielded similar tree topologies by ML and BI; with the ML tree shown in Fig. 4. The resulting trees revealed that *A. minutum* was polyphyletic comprising two clades. One clade consisted of ribotypes A and B, receiving high ML bootstrap support (94%) but low BI posterior probability, and formed a sister clade of *A. tamutum*, *A. ostenfeldii*, and *A. insuetum*. Another clade consisted of ribotypes C and D, with moderate ML bootstrap support (75%) but low BI posterior probability.

#### 3.2. Morphological characterization

##### 3.2.1. *Alexandrium minutum*

Dummy citations Figs 5,6,7,8,9,10 and 11

All strains of *A. minutum* were indistinguishable in morphology (Figs 5, 6, Fig. S1) although cell size was variable (14.4–30.4  $\mu\text{m}$  long, Table 4). Cells of strain TIO914 from the East China Sea had rounded epitheca and hypotheca, the hypotheca was divided into two parts by the deeply indented sulcus (Fig. 5A, B). Cells were often solitary and had thin and smooth thecal plates (Fig. 5B). The thecal plate pattern was Po, 4', 6'', 6c, 8s, 5''', 2'''. The apical pore complex was large with a comma shaped pore in the middle (Fig. 5C, E). The first apical plate (1') was rhomboidal in shape and directly contacted the pore plate (Po). There was a small ventral pore at the low suture between 1' and 4' plates (Fig. 5B). Plate 6'' was five-sided and narrow; the length/width ratio was about 1.9 ( $n = 5$ ). The anterior sulcal plate (Sa) was hook shaped and slightly longer than it was wide (Fig. 5B). The posterior sulcal plate (Sp) was wider than long (Fig. 5D). The two median plates (Sma and Smp) were much smaller than other sulcal plates (Fig. 5F).

Cell morphology of strain BK280604 from Malaysia was indistinguishable from strain TIO914 (Fig. 6). Cell morphology of strain AM-LYG from Yellow Sea, China was indistinguishable from strain TIO914 too, but the ventral pore was in the middle suture between plates 1' and 4' (Fig. 7). Cell morphology of Malaysian strains AmTm01 and AmTm02 were not examined in detail.

##### 3.2.2. *Alexandrium tamutum*

Cells of strain TIO598 from the East China Sea had rounded epitheca and hypotheca, with hypotheca divided into two parts by the deeply indented sulcus (Fig. 8A–C). Cells were often solitary and had thin and smooth thecal plates. The thecal plate pattern was Po, 4', 6'', 6c, 8s, 5''', 2'''. The apical pore complex was large with a comma shaped pore (Fig. 8D). Plate 1' was rhomboidal in shape and in direct contact with the pore plate (Po). There was a small ventral pore at the low suture between the 1' and 4' plates (Fig. 8B, D). Plate 6'' was five-sided and wide; the length/width ratio was about 0.8 ( $n = 4$ ) (Fig. 8B, D). Plate Sa was hook shaped and slightly longer than it was wide (Fig. 8B). Plate Sp was wider than long (Fig. 8E). The two median plates, Sma and Smp, were much smaller than other sulcal plates (Fig. 8F). Cell morphology of strain BK2703S1 from Malaysia was indistinguishable from strain TIO598 from China (Fig. S1), but it was much larger in size (22.2–33.5 vs 14.0–20.3  $\mu\text{m}$  long, Table 4).

#### 3.3. Toxin production of *Alexandrium minutum* and *A. tamutum*

No PSTs were detected in *A. tamutum* and *A. minutum* strain BK280604 (ribotype D). The limits of detection were 0.003, 0.042 and 0.048  $\text{pg cell}^{-1}$ , respectively (Table 1). However, PST production was confirmed in both ribotypes B (strains AM-LYG, AmTm01 and AmTm02) and C (strain TIO914) of *A. minutum*. GTX1/4 was dominant followed by GTX2/3 in the four above positive strains (Table 5). Traces of NEO and STX were also detected in strain AM-LYG (ribotype B) from Yellow Sea (Fig. 9, Table 5).

#### 3.4. Seasonal occurrence of *A. minutum*

For water samples from the Dongshan Bay, a total of 20,657 unique ZOTUs were obtained from the 10,532,740 processed reads. amongst them, 120 ZOTUs passed the similarity and coverage value thresholds. For water samples from Xiamen Harbour, a total of 6393 unique ZOTUs were obtained from the 11,081,177 processed reads. amongst them, 139 ZOTUs passed the similarity and coverage value thresholds. After randomly re-sampling to an equal sample size, total read abundances of ZOTUs annotated to *A. minutum* in samples of each month were obtained (Figs 10, 11).

Two ribotypes of *A. minutum* were detected although their relative abundances were very low at most stations. Only ribotype C occurred in the Dongshan Bay, but both ribotypes B and C were encountered in Xiamen Harbour. There were only a few reads of ribotype B but the abundance of ribotype C was much higher. The maximum relative abundances of ribotype C reached 10.6% and 4.8% at one station in Xiamen Harbour and Dongshan Bay, respectively. Ribotype C was more likely to occur in the summer and autumn (Figs 10, 11).

For sediment samples from the Dongshan Bay, a total of 226 unique ZOTUs were obtained from the 351,636 processed reads. Amongst them, 29 ZOTUs passed the similarity and coverage value thresholds. Only ribotype C of *A. minutum* was detected from one station with a relative abundance of 0.36%.

## 4. Discussion

#### 4.1. Cryptic diversity of *A. minutum* and *A. tamutum*

Cell morphology of all *A. minutum* strains examined in this study fit the original descriptions in terms of cell size, and shape of plate 6''

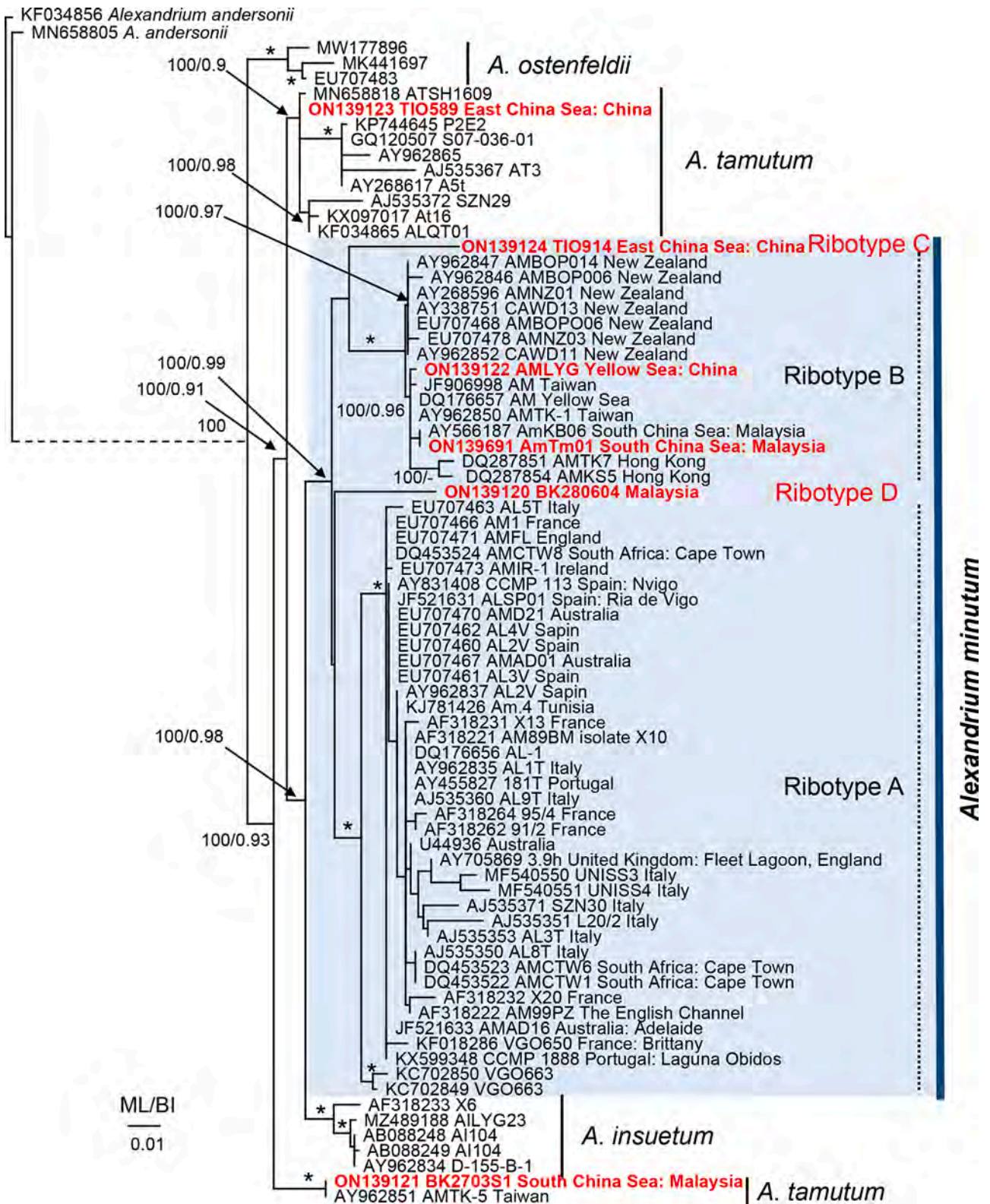


Fig. 3. Phylogenetic tree inferred from Maximum likelihood (ML) based on the *Alexandrium* LSU rDNA (D1–D3) sequences. Node labels in red and bold indicate new sequences obtained in this study. Branch lengths are drawn to scale, with the scale bar indicating the number of nucleotide substitutions per site. Node supports are bootstrap values of ML and Bayesian posterior probabilities (PP). Only ML values >50% and PP >0.9 are shown. Asterisk indicates ML bootstrap support value of 100% and a PP of 1.0.

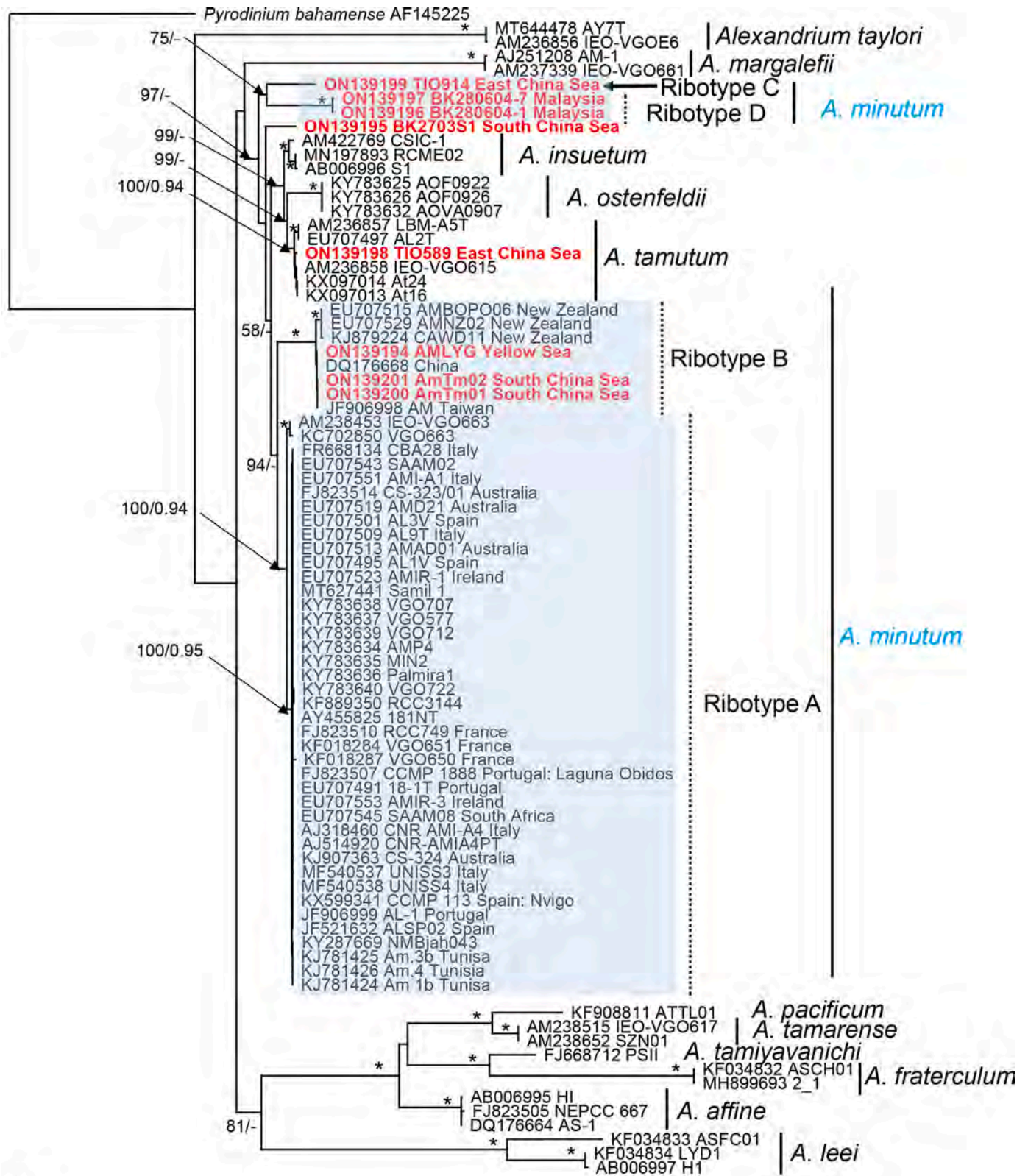
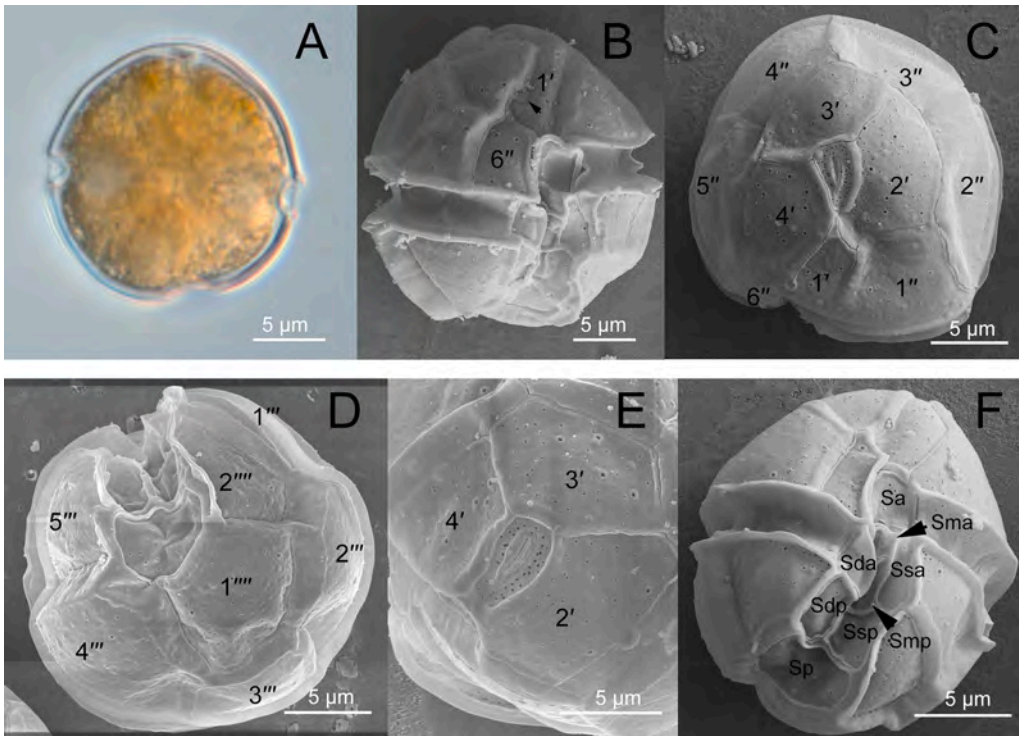
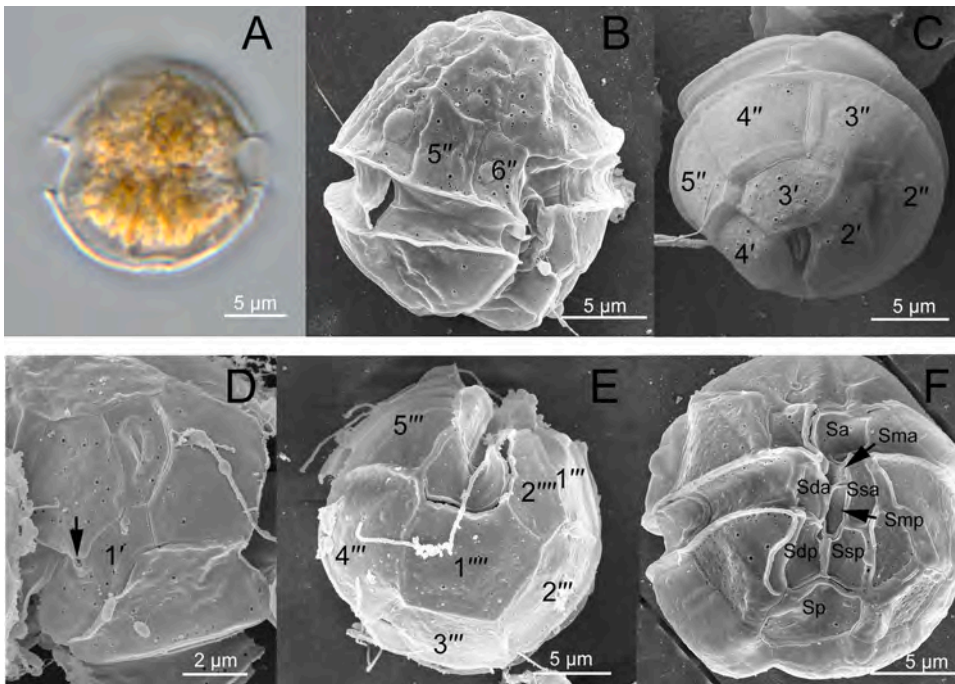


Fig. 4. Phylogenetic tree inferred from maximum likelihood (ML) based on the internal transcribed spacer (ITS) region sequences of *Alexandrium* species. Node labels in red and bold indicate new sequences obtained in this study. Node supports are bootstrap values of ML and Bayesian posterior probabilities (PP). Only ML values >50% and PP >0.9 are shown. Asterisk indicates ML bootstrap support value of 100% and a PP of 1.0.



**Fig. 5.** Light and scanning electron micrographs of cells of *Alexandrium minutum* strain TIO914. (A) A living cell; (B) Ventral view showing the ventral pore (arrow) and the sixth precingular plate (6''); (C) Apical view showing four apical plates (1'-4'), and six precingular plates (1''-6''). (D) Antapical view showing five postcingular plates (1'''-5''') and two antapical plates (1'''' and 2'''). (E) The apical pore plate with a comma shaped pore. (F) Ventral area of the sulcus showing anterior sulcal plate (Sa), right sulcal plates (Sda, Sdp), left sulcal plate (Ssa, Ssp), two median sulcal plates (Sma, Smp) and posterior sulcal plate (Sp).



**Fig. 6.** Light and scanning electron micrographs of cells of *Alexandrium minutum* strain BK280604. (A) A living cell; (B) Ventral view showing the sixth precingular plate (6''); (C) Apical view showing three apical plates (2'-4'), and four precingular plates (2''-5''). (D) Apical view showing the first apical plate (1'), the ventral pore (arrow) and the apical pore complex with a comma shaped pore. (E) Antapical view showing five postcingular plates (1'''-5''') and two antapical plates (1'''' and 2'''). (F) Ventral area of the sulcus showing anterior sulcal plate (Sa), right sulcal plates (Sda, Sdp), left sulcal plate (Ssa, Ssp), two median sulcal plates (Sma, Smp) and posterior sulcal plate (Sp).

(Table 4). Plate 1' was always narrow with a ventral pore present; the location of the ventral pore is in the lower part of suture between plates 1' and 4' in strains of ribotypes C and D, as also been reported in ribotype A (Hansen et al., 2003). Strain AM-LYG of ribotype B has a ventral pore in the middle part of suture between plates 1' and 4', similar to those of strains from New Zealand (MacKenzie and Berkett, 1997). However, a strain of ribotype B from Daya Bay has a ventral pore in the lower part of suture between plates 1' and 4' (Liu et al., 2021b), suggesting that this character is plastic and may not be suitable to differentiate amongst

these ribotypes. In fact, some strains from Denmark lack such a ventral pore (Hansen et al., 2003). All cells of *A. minutum* (ribotypes B-D) examined here have smooth surface, as has been reported previously (Su and Chiang, 1991; Lim et al., 2007b; Liu et al., 2021b). In contrast, some cells of ribotype A are heavily areolated (Hansen et al., 2003) and plate 1' of some cells are faintly reticulated (Balech, 1989).

Cysts of *A. minutum* were firstly reported from the surface sediment of the Port River, South Australia where blooms were observed (Bolch et al., 1991). The cysts were described as small (24-29 µm in diameter),

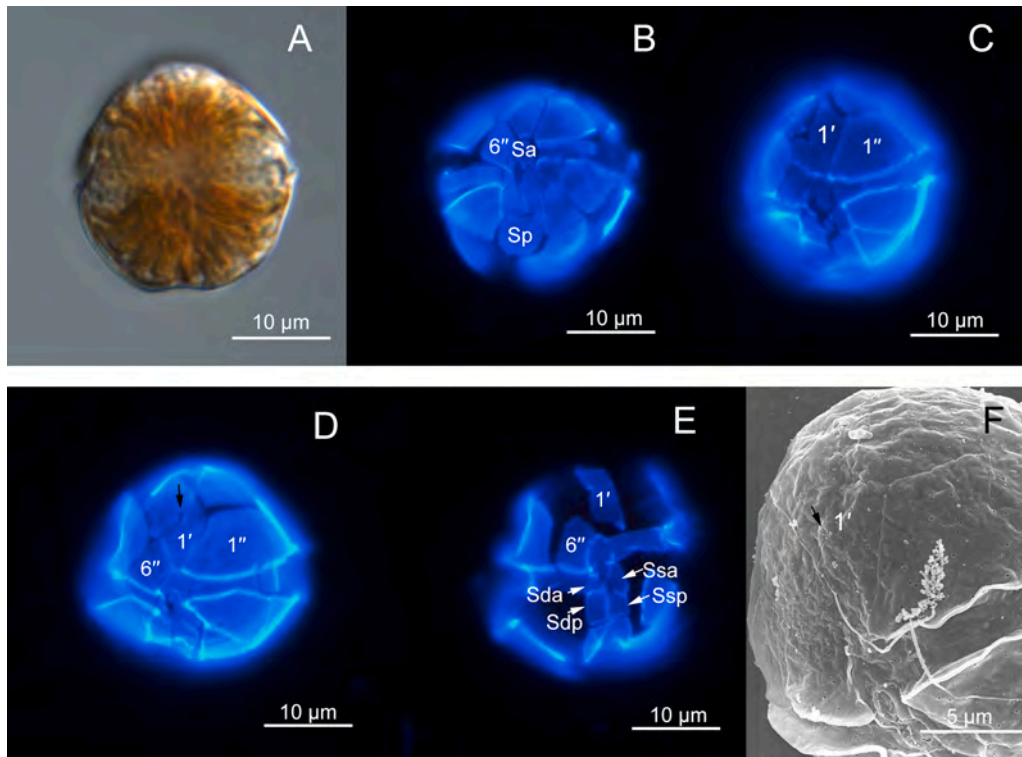


**Fig. 7.** Light, epifluorescence and scanning electron micrographs of cells of *Alexandrium minutum* strain AM-LYG. (A) A living cell; (B–D) Ventral view of calcofluor stained cells showing the ventral pore (arrow), anterior sulcal plate (Sa), posterior sulcal plate (Sp), the first apical plate (1') and the sixth precingular plates (6''); (E) Ventral area of the sulcus showing right sulcal plates (Sda, Sdp), and left sulcal plate (Ssa, Ssp); (F) Ventral view showing the ventral pore (arrow).

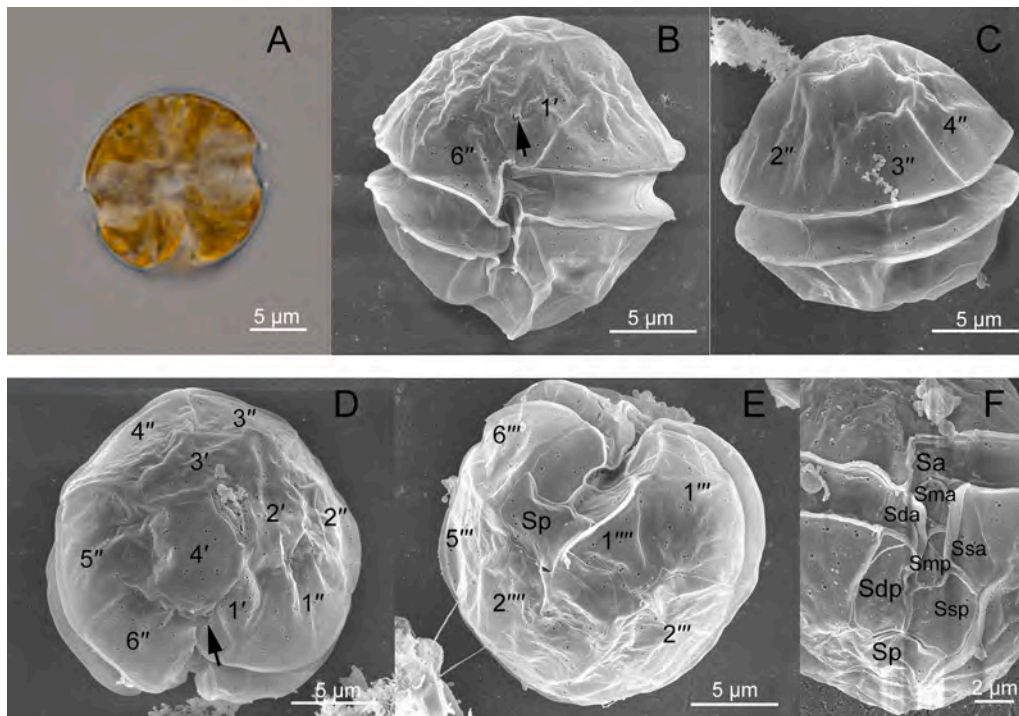


**Fig. 8.** Light and scanning electron micrographs of cells of *Alexandrium tamutum* strain TIO589. (A) A living cell; (B) Ventral view showing the ventral pore (arrow) and the sixth precingular plate (6''); (C) Dorsal view showing three precingular plates (2''-4''); (D) Apical view showing four apical plates (1'-4'), and six precingular plates (1''-6''); (E) Antapical view showing four postcingular plates and two antapical plates. (F) Ventral area of the sulcus showing anterior sulcal plate (Sa), right sulcal plates (Sda, Sdp), left sulcal plate (Ssa, Ssp), two median sulcal plates (Sma, Smp) and posterior sulcal plate (Sp).

round in apical view and hemispherical in lateral view. Such kind of cysts were later reported in the Mediterranean Sea (ribotype A; Garcés et al., 2004; Bravo et al., 2006), and from Peninsular Malaysia (ribotype B; Liow et al., 2021). Cysts of ribotype C were also detected through HTS metabarcoding in Dongshan Bay, although its morphology has not been

revealed by microscopy. Whether ribotype D also produces cysts remains to be determined and the trait has the potential to differentiate these ribotypes.

Cell morphology of two *A. tamutum* strains fits the original description and are indistinguishable from each other, too (Table 4). Cysts have

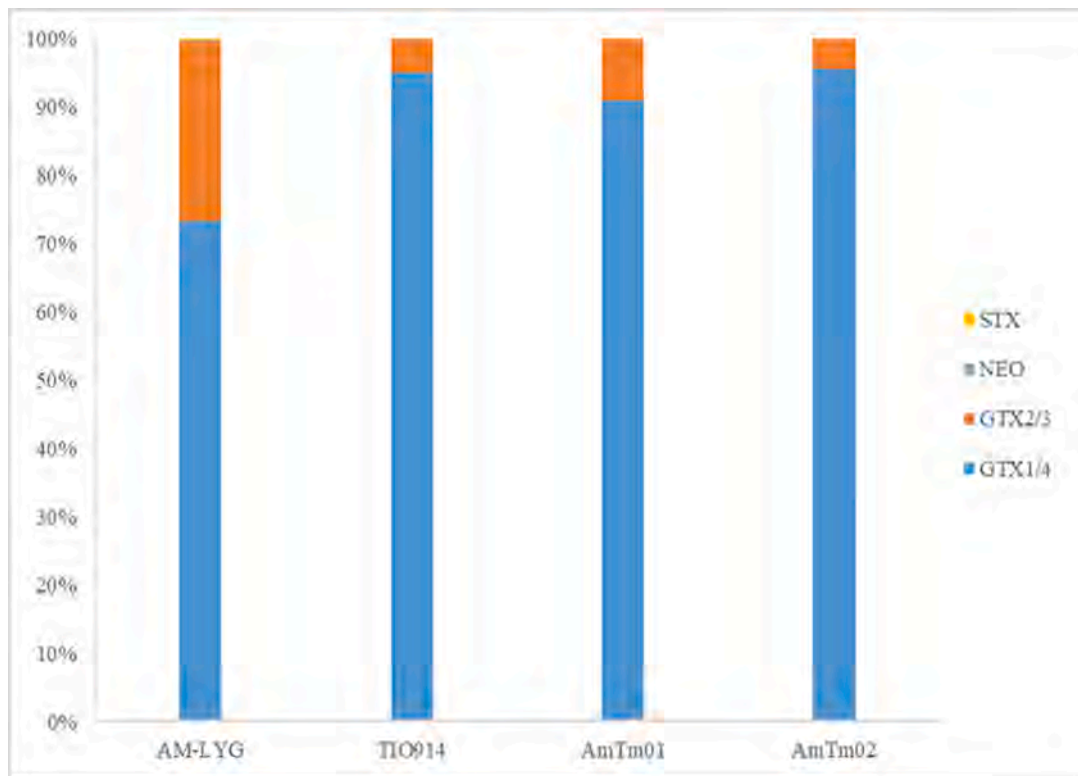


Fig. 9. Histograms showing the PST toxin composition (mol%) of *Alexandrium minutum* strains that showed toxicity: AM-LYG (Yellow Sea), TIO914 (East China Sea), AmTm01 and AmTm02 (South China Sea).

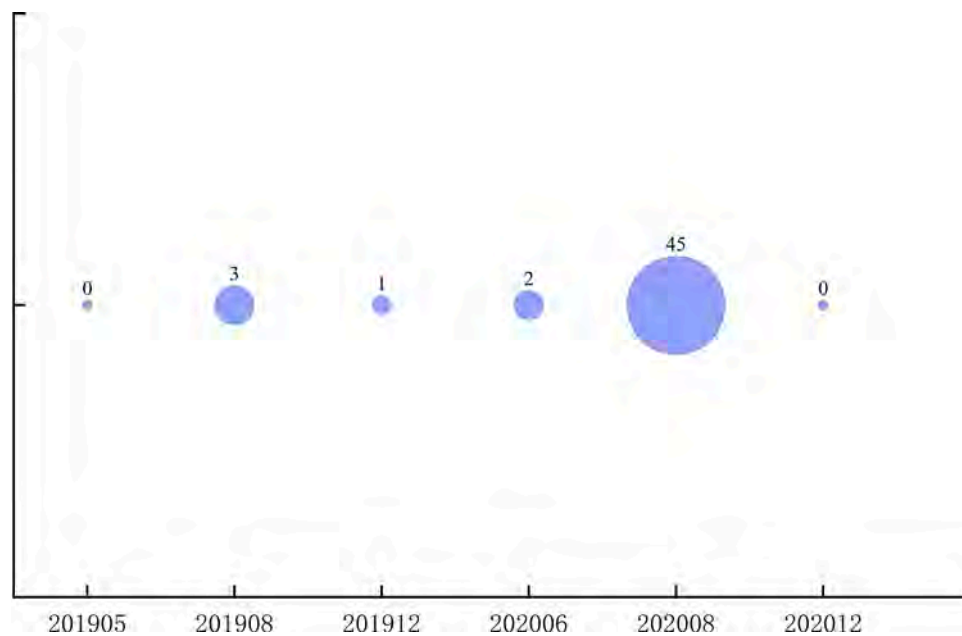
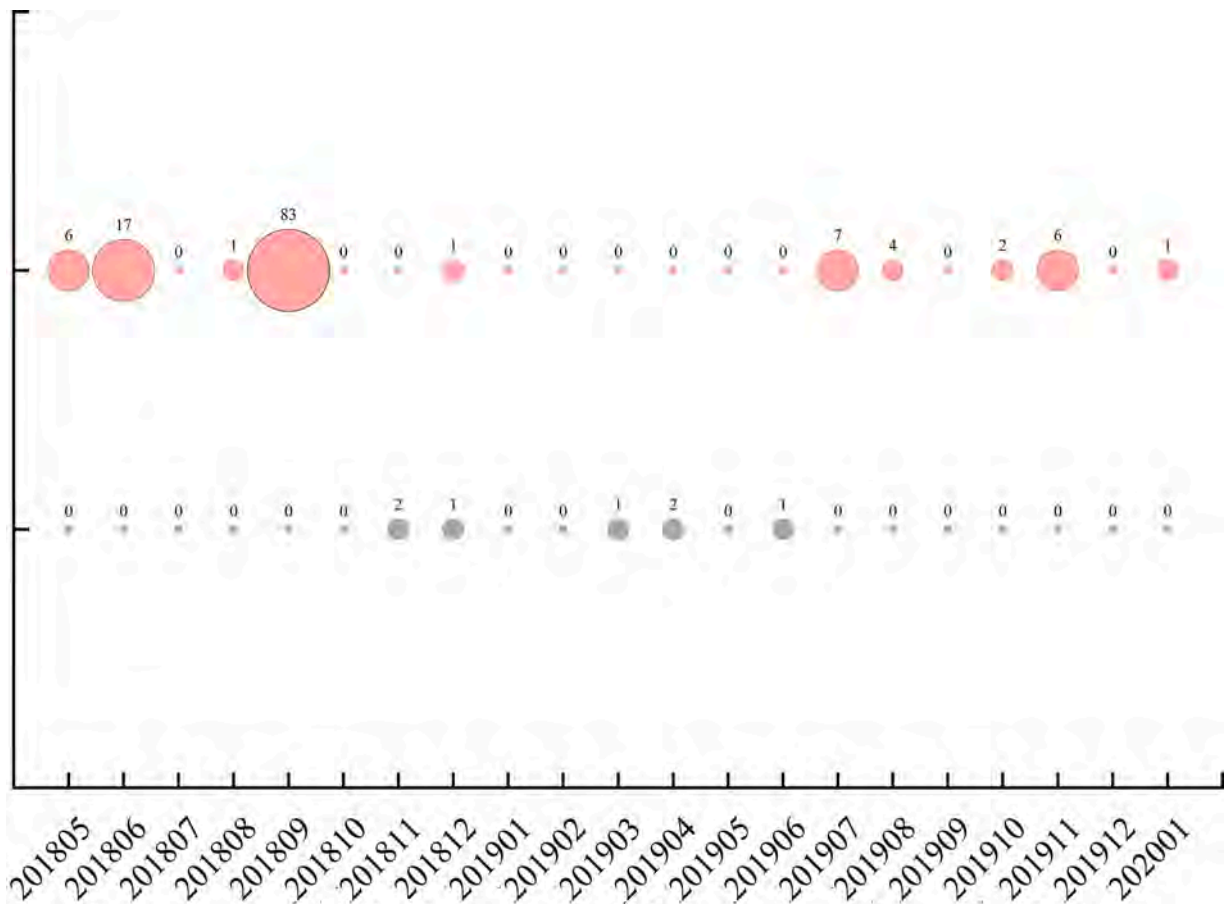


Fig. 10. Total read abundances of ZOTUs annotated to *Alexandrium minutum* ribotype C (blue circles) in Dongshan Bay from May 2019 to December 2020.

been reported in *A. tamutum* ribotype A (Montresor et al., 2004), but whether *A. tamutum* ribotype B also has a cyst stage is not clear. Cells of *A. tamutum* can be separated from those of *A. minutum* by the shape of plate 6', but both produce cysts of similar shape. It is therefore not possible to enumerate cysts directly during cyst mapping.

Both *A. minutum* and *A. tamutum* display high genetic diversification (Tables 2, 3), suggesting that each of them are cryptic species. The LSU and ITS sequence divergence amongst ribotypes of *A. minutum* can reach

10% and 25%, comparable to those amongst different *Alexandrium* species (Lim et al., 2015). It is reminiscent of the *Alexandrium tamarense* species complex, which was finally divided into five different species (John et al., 2014). However, more strains of *A. minutum* from Western Pacific are needed for detailed examination before taxonomic split is possible.



**Fig. 11.** Total read abundances of ZOTUs annotated to *Alexandrium minutum* ribotypes B (grey circles) and C (pink circles) in Xiamen Harbour from May 2018 to January 2020.

#### 4.2. Biogeography and seasonal occurrence of *A. minutum* ribotypes

Molecular phylogeny based on both LSU and ITS sequences revealed two ribotypes (A and B) of *A. minutum* as previously reported as global and Pacific clades (Lilly et al., 2005). The two new ribotypes (C and D) cluster together with other ribotypes in the LSU phylogeny but not in the ITS tree, raising concern that they may represent distinct species. Similar situation has been reported in *Azadinium spinosum* Elbrächter & Tillmann, which was tentatively named as *A. cf. spinosum* (Tillmann et al., 2021). But here we prefer to use ribotypes to name these new strains of *A. minutum*. Ribotype A has been reported in Europe, South Africa, and Australia, but cells were also detected in Chinhae Bay, Korea using a real-time quantitative PCR probe targeting LSU rDNA sequences of ribotype A (Park and Kang, 2009). The forward primer, however, matches the sequence of ribotype B; thus whether ribotype A or B is present in the water needed further confirmation. The other three ribotypes are only known in Asia Pacific and New Zealand so far, however, much wider distribution is expected since strains from elsewhere, such as Kingston Harbour, Jamaica (Ranston et al., 2007) have not been sequenced yet.

In our field observations on the occurrence of *A. minutum* ribotypes based on metabarcoding method, it is hard to determine the seasonal preference of ribotype B in Xiamen Harbour since only a few reads were detected. Blooms of *A. minutum* ribotype B developed in Lianyungang (Yellow Sea) in July, suggesting that it prefers warmer water (Lim et al., 2006; Tang et al., 2012). High abundance of ribotype C was recorded in Xiamen Harbour in the summer, also suggesting that it prefers warmer waters. Blooms of an unknown ribotype were observed in Southern Taiwan in winter (Hwang et al., 1999) and in Xiamen during

summertime (Lin, 1996; Gu et al., 2021), thus maybe representing different ecotypes as reported in *Akashiwo sanguinea* (Hirasaka) G. Hansen & Moestrup (Luo et al., 2017). Cells of *A. minutum* were reported to appear in Iwate, Japan in summer (Kaga et al., 2006), but its ribotype remains to be determined. Co-occurrence of several ribotypes of *A. minutum* in the waters poses monitoring challenges by molecular approaches previously designed, which is targeting single ribotype, either ribotype A or B (Touzet et al., 2009; Tang et al., 2012). In view of the high variance in the ribosomal DNA sequences amongst ribotypes of *A. minutum*, specific probes targeting the *sxtA4* gene might be promising to quantify toxic cells of *A. minutum*, such as the study that was applied to *A. catenella* (Murray et al., 2019).

#### 4.3. Toxin profiles of *A. minutum*

Toxin profiles of global populations of *A. minutum* are variable (Lewis et al., 2018), but ribotypes were not considered at that time. Our results showed that even within the same ribotype, for example ribotype B, toxin profiles appear to be related to their origin (Table 5). NEO and STX were only detected in strains from the Yellow Sea and New Zealand (MacKenzie and Berkett, 1997; present study). Toxin profiles of strains from Daya Bay, China and Penninsular Malaysia were distinct, as the former was dominated by GTX2/3 and the latter by GTX1/4 (Lim et al., 2006; Liu et al., 2021a; present study). Several strains of unknown ribotypes seem to follow this rule as well. Strains from Vietnam and the Gulf of Thailand produced predominantly GTX1/4 (Yoshida et al., 2000; Piumsomboon et al., 2001; Lim et al., 2007a), similar to strains AmTm01 and AmTm02 from Malaysia (Fig. 9). On the other hand, strains from Taiwan produced predominantly GTX2/3, similar to a strain from Daya

Bay, China (Table 5).

Strain TIO914 (ribotype C) produced predominantly GTX1/4, but ribotype B strains from close localities (e.g., Daya Bay) produced mainly GTX2/3 (Liu et al., 2021b), suggesting that genetic changes in the ribotypes are accompanied by physiological differentiation. Ribotype C prefers warmer waters thus the presence in the water might be the source of GTX1/4 detected in the phytoplankton samples from a station adjacent to the Changjiang River in the summer (Liu et al., 2020b). Although *Alexandrium pacificum* and *Gymnodinium catenatum* Graham have been reported in this area and were suspected to be the species contributing to the toxicity, they produced predominantly C1/2 with little or no GTX1/4 (Liu et al., 2020a, 2021a). Strain BK280604 (ribotype D) did not produce any detectable toxin (<0.048 pg cell<sup>-1</sup>), comparable to the detection limit (0.035 pg cell<sup>-1</sup>) of a nontoxic strain from Scotland (Brown et al., 2010). However, this does not necessarily mean that ribotype D is nontoxic, since both toxic and nontoxic strains were found within ribotypes A and B (Lilly et al., 2005; Yang et al., 2010). It will be interesting to investigate whether this nontoxic strain also has the sxtA4 gene and how many copies are present. Previously only one copy was found in two non-toxic ribotype A strains of *A. minutum* as compared to 9–187 gene copies in the toxic strains (Geffroy et al., 2021).

## 5. Conclusions

Our very limited sampling in the coastal waters of China and Malaysia unveiled the unexpected diversity within the toxic dinophyte *A. minutum*. Four ribotypes of *A. minutum* were identified; two of them correspond to the previously defined global and Pacific clades, but the other two ribotypes were proven to be novel. Currently, Western Pacific *A. minutum* strains with the molecular sequences available are still limited, thus future efforts are needed to reveal the biogeography of these novel ribotypes. All examined *A. minutum* strains are toxic and produce carbamoyl toxins dominated by GTX1/4 except one strain of ribotype D. This contrasts with the common toxic PSTs producing *A. pacificum* and *Gymnodinium catenatum* in the region, which produce predominantly less potent C1/2 toxin (Liu et al., 2020a, 2021a), highlighting the potential risk of shellfish poisoning by *A. minutum* and the importance of routine monitoring.

## Declaration of Competing Interest

The authors declare that they have no known competing financial interests or personal relationships that could have appeared to influence the work reported in this paper. The authors declare the following financial interests/personal relationships which may be considered as potential competing interests:

## Acknowledgements

This work was supported by National Natural Science Foundation of China (42030404), the National Key Research and Development Program of China (2019YFE0124700), Asian Cooperation Fund Project-Study on Typical Bay Ecological Protection and Management Demonstration, Fund Project for Marine and Fishery Protection and Development in Fujian Province (FZJZ-2021-1); and the Ministry of Higher Education of Malaysia HICOE (IOES-2014C) and LRGS (LRGS/1/2020/UMT/01/1/3) to P.T.Lim. We thank two anonymous reviewers for constructive suggestions and Zhaohe Luo for technical support.

## Supplementary materials

Supplementary material associated with this article can be found, in the online version, at [doi:10.1016/j.hal.2022.102238](https://doi.org/10.1016/j.hal.2022.102238).

## References

- Abdenadher, M., Hamza, A., Fekih, W., Hannachi, I., Bellaaj, A.Z., Bradai, M.N., Aleya, L., 2012. Factors determining the dynamics of toxic blooms of *Alexandrium minutum* during a 10-year study along the shallow southwestern Mediterranean coasts. *Estuar. Coast. Shelf Sci.* 106, 102–111.
- Adachi, M., Sako, Y., Ishida, Y., 1996. Analysis of *Alexandrium* (Dinophyceae) species using sequences of the 5.8S ribosomal DNA and internal transcribed spacer regions. *J. Phycol.* 32 (3), 424–432.
- Anderson, D.M., Alpermann, T.J., Cembella, A.D., Collos, Y., Masseret, E., Montresor, M., 2012. The globally distributed genus *Alexandrium*: multifaceted roles in marine ecosystems and impacts on human health. *Harmful Algae* 14, 10–35.
- Balech, E., 1980. On the Thecal Morphology of Dinoflagellates With Special Emphasis On Circular and Sulcal plates. *Anales del Centro de Ciencias del Mar y Limnología, Universidad Nacional Autonomía de México* 7, 57–68.
- Balech, E., 1989. Redescription of *Alexandrium minutum* Halim (Dinophyceae) type species of the genus *Alexandrium*. *Phycologia* 28 (2), 206–211.
- Balech, E., 1995. The Genus *Alexandrium* Halim (Dinoflagellata). *Sherkin Island Marine Station, Sherkin Island, Co. Cork, Ireland*.
- Baula, I.U., Azanza, R.V., Fukuyo, Y., Siringan, F.P., 2011. Dinoflagellate cyst composition, abundance and horizontal distribution in Bolinao, Pangasinan, Northern Philippines. *Harmful Algae* 11, 33–44.
- Boc, A., Diallo, A.B., Makarenkov, V., 2012. T-REX: a web server for inferring, validating and visualizing phylogenetic trees and networks. *Nucleic. Acids. Res.* 40 (W1), W573–W579.
- Bolch, C., Blackburn, S., Cannon, J., Hallegraef, G., 1991. The resting cyst of the red-tide dinoflagellate *Alexandrium minutum* (Dinophyceae). *Phycologia* 30 (2), 215–219.
- Bravo, I., Garcés, E., Diogène, J., Fraga, S., Sampedro, N., Figueroa, R.I., 2006. Resting cysts of the toxigenic dinoflagellate genus *Alexandrium* in recent sediments from the Western Mediterranean coast, including the first description of cysts of *A. kuteranae* and *A. peruvianum*. *Eur. J. Phycol.* 41 (3), 293–302.
- Bravo, I., Vila, M., Masó, M., Figueroa, R.I., Ramilo, I., 2008. *Alexandrium catenella* and *Alexandrium minutum* blooms in the Mediterranean Sea: toward the identification of ecological niches. *Harmful Algae* 7 (4), 515–522.
- Brown, L., Bresnan, E., Graham, J., Lacaze, J.P., Turrell, E., Collins, C., 2010. Distribution, diversity and toxin composition of the genus *Alexandrium* (Dinophyceae) in Scottish waters. *Eur. J. Phycol.* 45 (4), 375–393.
- Chapelle, A., Le Gac, M., Labry, C., Siano, R., Quere, J., Caradec, F., Le Bec, C., Nezan, E., Doner, A., Gouriou, J., 2015. The Bay of Brest (France), a new risky site for toxic *Alexandrium minutum* blooms and PSP shellfish contamination. *Harmful Algae News* 51, 4–5.
- Daugbjerg, N., Hansen, G., Larsen, J., Moestrup, Ø., 2000. Phylogeny of some of the major genera of dinoflagellates based on ultrastructure and partial LSU rDNA sequence data, including the erection of three new genera of unarmoured dinoflagellates. *Phycologia* 39 (4), 302–317.
- Delgado, M., Estrada, M., Camp, J., Fernández, J.V., Santmartí, M., Lletí, C., 1990. Development of a toxic *Alexandrium minutum* Halim (Dinophyceae) bloom in the harbour of Sant Carles de la Rapita (Ebro Delta, northwestern Mediterranean). *Sci. Mar.* 54, 1–7.
- Edgar, R.C., 2013. UPPARSE: highly accurate OTU sequences from microbial amplicon reads. *Nat. Methods* 10 (10), 996–998.
- Edgar, R.C., Flyvbjerg, H., 2015. Error filtering, pair assembly and error correction for next-generation sequencing reads. *Bioinformatics* 31 (21), 3476–3482.
- Fensome, R.A., Taylor, F.J.R., Norris, G., Sarjeant, W.A.S., Wharton, D.I., Williams, G.L., 1993. A classification of fossil and living dinoflagellates. *Micropaleontology Special Publication* 7, 1–245.
- Fraga, S., Sampedro, N., Larsen, J., Moestrup, Ø., Calado, A.J., 2015. Arguments against the proposal 2302 by John & al. to reject the name *Gonyaulax catenella* (*Alexandrium catenella*). *Taxon* 64, 634–635.
- Fritz, L., Triemer, R., 1985. A rapid simple technique utilizing calcofluor white M2R for the visualization of dinoflagellate thecal plates. *J. Phycol.* 21 (4), 662–664.
- Fu, Z., Piumsomboon, A., Punnarak, P., Uttayarnmanee, P., Leaw, C.P., Lim, P.T., Wang, A., Gu, H., 2021. Diversity and distribution of harmful microalgae in the Gulf of Thailand assessed by DNA metabarcoding. *Harmful Algae* 106, 102063.
- Galluzzi, L., Penna, A., Bertozzini, E., Vila, M., Garcés, E., Magnani, M., 2004. Development of a real-time PCR assay for rapid detection and quantification of *Alexandrium minutum* (a dinoflagellate). *Appl. Environ. Microbiol.* 70 (2), 1199–1206.
- Garcés, E., Bravo, I., Vila, M., Figueroa, R.I., Masó, M., Sampedro, N., 2004. Relationship between vegetative cells and cyst production during *Alexandrium minutum* bloom in Arenys de Mar harbour (NW Mediterranean). *J. Plankton Res.* 26 (6), 637–645.
- Geffroy, S., Lechat, M.-M., Le Gac, M., Rovillon, G.-A., Marie, D., Bigeard, E., Malo, F., Amzil, Z., Guillou, L., Caruana, A.M.N., 2021. From the sxtA4 Gene to Saxitoxin Production: what Controls the Variability Among *Alexandrium minutum* and *Alexandrium pacificum* Strains? *Front. Microbiol.* 12 (341).
- Gu, H., Wu, Y., Lü, S., Lu, D., Tang, Y.Z., Qi, Y., 2021. Emerging harmful algal bloom species over the last four decades in China. *Harmful Algae*, 102059.
- Guallar, C., Bacher, C., Chapelle, A., 2017. Global and local factors driving the phenology of *Alexandrium minutum* (Halim) blooms and its toxicity. *Harmful Algae* 67, 44–60.
- Guiry, M.D., Guiry, G.M. *AlgaeBase*. World-wide Electronic Publication, National University of Ireland, Galway. <https://www.algaebase.org>; searched on January 6, 2022.
- Guillard, R.R.L., Ryther, J.H., 1962. Studies of marine planktonic diatoms. I. *Cyclotella nana* Hustedt and *Detonula confervacea* Cleve. *Can. J. Microbiol.* 8, 229–239.
- Halim, Y., 1960. *Alexandrium minutum* nov. g. nov. sp. dinoflagellé provocant des 'eaux rouges'. *Vie Milieu* 11 (1), 102–105.

- Hall, T.A., 1999. BioEdit: a user-friendly biological sequence alignment editor and analysis program for Windows 95/98/NT. In: Series, N.A.S. (Ed.), pp. 95–98.
- Hallegraeff, G., Steffensen, D., Wetherbee, R., 1988. Three estuarine Australian dinoflagellates that can produce paralytic shellfish toxins. *J. Plankton Res.* 10 (3), 533–541.
- Hansen, G., Daugbjerg, N., Franco, J., 2003. Morphology, toxin composition and LSU rDNA phylogeny of *Alexandrium minutum* (Dinophyceae) from Denmark, with some morphological observations on other European strains. *Harmful Algae* 2 (4), 317–335.
- Hwang, D.-F., Tsai, Y.-H., Liao, H.-J., Matsuoka, K., Noguchi, T., Jeng, S.-S., 1999. Toxins of the dinoflagellate *Alexandrium minutum* Halim from the coastal waters and aquaculture ponds in southern Taiwan. *Fish. Sci.* 65 (1), 171–172.
- John, U., Litaker, R.W., Montresor, M., Murray, S., Brosnahan, M.L., Anderson, D.M., 2014. Formal revision of the *Alexandrium tamarensis* species complex (Dinophyceae) taxonomy: the introduction of five species with emphasis on molecular-based (rDNA) classification. *Protist* 165 (6), 779–804.
- Kaga, S., Sekiguchi, K., Yoshida, M., Ogata, T., 2006. Occurrence and toxin production of *Alexandrium* spp. (Dinophyceae) in coastal waters of Iwate Prefecture. *Japan. Nippon Suisan Gakkaishi* 72 (6), 1068–1076.
- Katoh, K., Standley, D.M., 2013. MAFFT multiple sequence alignment software versions 7: improvements in performance and usability. *Mol. Biol. Evol.* 30 (4), 772–780.
- Lau, W.L.S., Law, K., Liow, G.R., Hii, K.S., Usup, G., Lim, P.T., Leaw, C.P., 2017. Life-history stages of natural bloom populations and the bloom dynamics of a tropical Asian ribotype of *Alexandrium minutum*. *Harmful Algae* 70, 52–63.
- Lebour, M.V., 1925. The dinoflagellates of the northern seas. Marine Biological Association of the United Kingdom, Plymouth (UK).
- Lewis, A.M., Coates, L.N., Turner, A.D., Percy, L., Lewis, J., 2018. A review of the global distribution of *Alexandrium minutum* (Dinophyceae) and comments on ecology and associated paralytic shellfish toxin profiles, with a focus on Northern Europe. *J. Phycol.* 54 (5), 581–598.
- Lilly, E., Halanych, K., Anderson, D., 2005. Phylogeny, biogeography, and species boundaries within the *Alexandrium minutum* group. *Harmful Algae* 4 (6), 1004–1020.
- Lim, A.S., Jeong, H.J., Kim, J.H., Lee, S.Y., 2015. Description of the new phototrophic dinoflagellate *Alexandrium pohangense* sp. nov. from Korean coastal waters. *Harmful Algae* 46, 49–61.
- Lim, P.T., Leaw, C.P., Usup, G., 2004. First incidence of paralytic shellfish poisoning on the east coast of Peninsular Malaysia. *Marine science into the new millennium: new perspectives and challenges* 661–667.
- Lim, P.T., Leaw, C.P., Usup, G., Kobiyama, A., Koike, K., Ogata, T., 2006. Effects of light and temperature on growth, nitrate uptake, and toxin production of two tropical dinoflagellates: *Alexandrium tamiyavanichii* and *Alexandrium minutum* (Dinophyceae). *J. Phycol.* 42 (4), 786–799.
- Lim, P.T., Ogata, T., 2005. Salinity effect on growth and toxin production of four tropical *Alexandrium* species (Dinophyceae). *Toxicol.* 45 (6), 699–710.
- Lim, P.T., Sato, S., Van Thuoc, C., Huyen, N.T.M., Takata, Y., Yoshida, M., Kobiyama, A., Koike, K., Ogata, T., 2007a. Toxic *Alexandrium minutum* (Dinophyceae) from Vietnam with new gonyautoxin analogue. *Harmful Algae* 6 (3), 321–331.
- Lim, P.T., Leaw, C.P., Ogata, T., 2007b. Morphological variation of two *Alexandrium* responsible for paralytic shellfish poisoning in Southeast Asia. *Bot. Mar.* 50, 14–21.
- Lim, P.T., Leaw, C.P., Kobiyama, A., Ogata, T., 2010. Growth and toxin production of tropical *Alexandrium minutum* Halim (Dinophyceae) under various nitrogen to phosphorus ratio. *J. Appl. Phycol.* 22, 203–210.
- Lin, Y., 1996. Red tide caused by a marine toxic dinoflagellate, *Alexandrium tamarensis* (Lebour) Balech, in shrimp ponds in Xiamen. *Taiwan Strait* 15 (1), 16–18 (In Chinese with English abstract).
- Liow, G.R., Lau, W.L.S., Law, I.K., Gu, H., Leaw, C.P., Lim, P.T., 2021. Sexual processes and life cycle transitions of the tropical Pacific *Alexandrium minutum* (Dinophyceae). *Phycol. Res.* 69 (3), 188–199.
- Liu, M., Gu, H., Krock, B., Luo, Z., Zhang, Y., 2020a. Toxic dinoflagellate blooms of *Gymnodinium catenatum* and their cysts in Taiwan Strait and their relationship to global populations. *Harmful Algae* 97, 101868.
- Liu, M., Zheng, J., Krock, B., Ding, G., MacKenzie, L., Smith, K.F., Gu, H., 2021a. Dynamics of the Toxic Dinoflagellate *Alexandrium pacificum* in the Taiwan Strait and Its Linkages to Surrounding Populations. *Water (Basel)* 13 (19), 2681.
- Liu, Y., Chen, Z., Gao, Y., Zou, J., Lu, S., Zhang, L., 2021b. Identifying the Source Organisms Producing Paralytic Shellfish Toxins in a Subtropical Bay in the South China Sea. *Environ. Sci. Technol.* 55 (5), 3124–3135.
- Liu, Y., Dai, L., Chen, Z.F., Geng, H.X., Lin, Z.R., Zhao, Y., Zhou, Z.X., Kong, F.Z., Yu, R. C., Zhou, M.J., 2020b. Spatiotemporal variation of paralytic shellfish toxins in the sea area adjacent to the Changjiang River estuary. *Environ. Pollut.* 259, 113730.
- Luo, Z., Yang, W., Leaw, C.P., Pospelova, V., Bilien, G., Liow, G.R., Lim, P.T., Gu, H., 2017. Cryptic diversity within the harmful dinoflagellate *Akashiwo sanguinea* in coastal Chinese waters is related to differentiated ecological niches. *Harmful Algae* 66, 88–96.
- MacKenzie, L., Berkett, N., 1997. Cell morphology and PSP-toxin profiles of *Alexandrium minutum* in the Marlborough Sounds. *New Zealand. N. Z. J. Mar. Freshwat. Res.* 31 (3), 403–409.
- Medlin, L., Elwood, H.J., Stickel, S., Sogin, M.L., 1988. The characterization of enzymatically amplified eukaryotic 16S-like rRNA-coding regions. *Gene* 71 (2), 491–499.
- Montresor, M., John, U., Beran, A., Medlin, L., 2004. *Alexandrium tamutum* sp. nov. (Dinophyceae): a new, non-toxic species in the genus *Alexandrium*. *J. Phycol.* 40 (2), 398–411.
- Murray, S.A., Ruvindy, R., Kohli, G.S., Anderson, D.M., Brosnahan, M.L., 2019. Evaluation of sxtA and rDNA qPCR assays through monitoring of an inshore bloom of *Alexandrium catenella* Group 1. *Sci. Rep.* 9 (1), 1–12.
- Oshima, Y., Hirota, M., Yasumoto, T., Hallegraeff, G.M., Blackburn, S.I., Steffensen, D.A., 1989. Production of paralytic shellfish toxins by the dinoflagellate *Alexandrium minutum* Halim from Australia. *Nippon Suisan Gakkaishi* 55 (5), 925.
- Park, T.G., Kang, Y.S., 2009. Temporal Changes in Abundances of the Toxic Dinoflagellate *Alexandrium minutum* (Dinophyceae) in Chinhae Bay. *Korea. J. Environ. Sci. Int.* 18 (12), 1331–1338.
- Pitcher, G., Cembella, A., Joyce, L., Larsen, J., Probyn, T., Sebastián, C.R., 2007. The dinoflagellate *Alexandrium minutum* in Cape Town harbour (South Africa): bloom characteristics, phylogenetic analysis and toxin composition. *Harmful Algae* 6 (6), 823–836.
- Piumsomboon, A., Songroop, C., Kungsowan, A., Polpunth, P., 2001. Species of the dinoflagellate genus *Alexandrium* (Gonyaulacales) in the Gulf of Thailand. In: Hallegraeff, G.M., Blackburn, S.I., Bolch, C.J., Lewis, R.J. (Eds.), *Harmful Algal Blooms*. IOC of UNESCO, 2000, pp. 12–15.
- Posada, D., 2008. jModelTest: phylogenetic model averaging. *Mol. Biol. Evol.* 25 (7), 1253–1256.
- Ranston, E.R., Webber, D.F., Larsen, J., 2007. The first description of the potentially toxic dinoflagellate, *Alexandrium minutum* in Hunts Bay, Kingston Harbour, Jamaica. *Harmful Algae* 6 (1), 29–47.
- Rognes, T., Flouri, T., Nichols, B., Quince, C., Mahé, F., 2016. VSEARCH: a versatile open source tool for metagenomics. *PeerJ* 4, e2584.
- Ronquist, F., Huelsenbeck, J.P., 2003. MrBayes 3: bayesian phylogenetic inference under mixed models. *Bioinformatics* 19 (12), 1572–1574.
- Santos, M., Costa, P.R., Porteiro, F.M., Moita, M.T., 2014. First report of a massive bloom of *Alexandrium minutum* (Dinophyceae) in middle North Atlantic: a coastal lagoon in S. Jorge Island, Azores. *Toxicol.* 90, 265–268.
- Silveira, S., Kawakami, Y., Kanno, N., Kasai, H., Shiimoto, A., Katakura, S., Nagai, S., 2019. Toxic HAB species from the Sea of Okhotsk detected by a metagenetic approach, seasonality and environmental drivers. *Harmful Algae* 87, 101631.
- Stamatakis, A., 2006. RAxML-VI-HPC: maximum likelihood-based phylogenetic analyses with thousands of taxa and mixed models. *Bioinformatics* 22 (21), 2688–2690.
- Su, H., Chiang, Y., 1991. Dinoflagellates collected from aquaculture ponds in southern Taiwan. *Jpn. J. Phycol.* 39, 227–237.
- Tang, X., Yu, R., Zhou, M., Yu, Z., 2012. Application of rRNA probes and fluorescence in situ hybridization for rapid detection of the toxic dinoflagellate *Alexandrium minutum*. *Chin. J. Oceanol. Limnol.* 30 (2), 256–263.
- Tillmann, U., Wietkamp, S., Gu, H., Krock, B., Salas, R., Clarke, D., 2021. Multiple New Strains of Amphidomataceae (Dinophyceae) from the North Atlantic Revealed a High Toxin Profile Variability of *Azadinium spinosum* and a New Non-Toxicigenic Az. cf. *spinosum*. *Microorganisms* 9 (1), 134.
- Touzet, N., Franco, J.M., Raine, R., 2007. Characterization of nontoxic and toxin-producing strains of *Alexandrium minutum* (Dinophyceae) in Irish coastal waters. *Appl. Environ. Microbiol.* 73 (10), 3333–3342.
- Touzet, N., Keady, E., Raine, R., Maher, M., 2009. Evaluation of taxa-specific real-time PCR, whole-cell FISH and morphotaxonomy analyses for the detection and quantification of the toxic microalgae *Alexandrium minutum* (Dinophyceae), Global Clade ribotype. *FEMS Microbiol. Ecol.* 67 (2), 329–341.
- Usup, G., Pin, L.C., Ahmad, A., Teen, L.P., 2002. *Alexandrium* (Dinophyceae) species in Malaysian waters. *Harmful Algae* 1 (3), 265–275.
- Vila, M., Giacobbe, M.G., Masó, M., Gangemi, E., Penna, A., Sampedro, N., Azzaro, F., Camp, J., Galluzzi, L., 2005. A comparative study on recurrent blooms of *Alexandrium minutum* in two Mediterranean coastal areas. *Harmful Algae* 4 (4), 673–695.
- Whedon, W.F., Kofoid, C.A., 1936. *Dinoflagellata of the San Francisco Region*. University of California Press.
- Yang, I., John, U., Beszteri, S., Glöckner, G., Krock, B., Goesmann, A., Cembella, A., 2010. Comparative gene expression in toxic versus non-toxic strains of the marine dinoflagellate *Alexandrium minutum*. *BMC Genomics* 11 (1), 248.
- Yoshida, M., Ogata, T., Van Thuoc, C., Matsuoka, K., Fukuyo, Y., Hoi, N.C., Kodama, M., 2000. The first finding of toxic dinoflagellate *Alexandrium minutum* in Vietnam. *Fish. Sci.* 66 (1), 177–179.
- Yuki, K., 1994. First report of *Alexandrium minutum* Halim (Dinophyceae) from Japan. *Jpn. J. Phycol.* 42, 425–430.